Journal of Solid State Chemistry **168,** 563–572 (2002)
doi:10.1006/jssc.2002.9753

Two New Families of Charge Transfer Solids Based on $[M(mnt)_2]^{n-}$ and the Donors BMDT-TTF and EDT-TTF: Conducting and Magnetic Properties

M. Mas-Torrent,* H. Alves,† E. B. Lopes,† M. Almeida,† K. Wurst,‡ J. Vidal-Gancedo,* J. Veciana,* and C. Rovira*,[1]

*Institut de Ciencia de Materials de Barcelona, CSIC, Campus Universitari de Bellaterra, E-08193 Cerdanyola, Spain; †Departmentode. Química, Instituto Tecnológico e Nuclear, P-2686-953 Sacavém Codex, Portugal; and ‡Instintitut für Allgemeine Anorganische und Theoretische Chemie, Universität Innsbruck, Innrain 52a, A-6020 Innsbruck, Austria

Received January 8, 2002; in revised form April 10, 2002; accepted April 19, 2002

Two new families of charge transfer solids based on transition metal bis-maleonitrile dithiolate complexes $[M(mnt)_2]^{n-}$ and two tetrathiatulvalene (TTF) derivatives containing external sulfur atoms have been synthesized and characterized as (BMDT-TTF)$_2$[M(mnt)$_2$] and (EDT-TTF)[M(mnt)$_2$], where BMDT-TTF stands for bis(methylenedithio)-tetrathiafulvalene, EDT-TTF for ethylenedithio-tetrathiafulvalene and M = Au, Pt and Ni. The salts of the series (BMDT-TTF)$_2$[M(mnt)$_2$] are quasi-isostructural and crystallize forming mixed ADDA stacks along $a+b$. In the (BMDT-TTF)$_2$[Au(mnt)$_2$] salt, the anion complex is diamagnetic and has a formal charge of -1, whereas in Ni salt the anion has a charge of -2, being also diamagnetic. The magnetic properties of the Au salt follow a 1D antiferromagnetic Heisenberg model modified with a molecular field. The salt with Ni displays very strong antiferromagnetic interactions. The (EDT-TTF)[M(mnt)$_2$] salts with M = Ni and Pt are isostructural and crystallize forming alternated DADA stacks. The anions, with a formal charge of -1, are paramagnetic with a spin $\frac{1}{2}$. Their magnetic susceptibility can be successfully simulated within the antiferromagnetic uniform chain model of Heisenberg. Lastly, (EDT-TTF)[Au(mnt)$_2$] crystallizes in the triclinic space group P(-1) forming also alternated stacks along c in which the EDT-TTF molecules are 50% disordered. © 2002 Elsevier Science (USA)

Key Words: **charge transfer salt; magnetic susceptibility; conductivity; crystal structure.**

1. INTRODUCTION

Since the discovery of metallic properties in molecular organic compounds, a large variety of such materials based on planar π-electron donor molecules has been synthesized and characterized by a wide range of transport properties from insulating and semiconducting to metallic and superconducting (1). More recently, substantial efforts have been devoted to preparing molecule-based magnets in which the localized magnetic moments co-exist with the conducting electrons. The work in this direction has led to the design of hybrid materials formed by two molecular networks combining metal complexes, that act as components with localized magnetic moments, with π-electron donor molecules, that furnish the pathway for electronic conductivity (2,3).

The (per)$_2$[M(mnt)$_2$] (per = perylene; mnt = maleonitrile dithiolate and M = ransition metal) is one of the oldest known families in which the conduction electrons and the localized spins reside in two different stacks co-existing and interacting in the same solid (4,5). The crystal structure of these compounds can be described as regular stacks of partially oxidized perylene molecules, $(per)^{0.5+}$, surrounded by regular stacks of $[M(mnt)_2]^-$ counterions. The number of perylene stacks is twice that of $M(mnt)_2$ stacks but the inter-stack perylene–perylene interactions are extremely small compared with the strong intra-stack interactions and, as a consequence, these compounds are metals with a very strong 1D character. In order to establish interactions between pairs of donor stacks and, hence, achieve a ladder-type molecular organic compound, previously in our group a new family of salts was prepared replacing the perylene molecules with the donor dithiopheno-tetrathiafulvalene (DT-TTF), which incorporates six peripheral sulfur atoms (6). Depending on the nature of the transition metal M, different conducting and magnetic properties were observed. In the (DT-TTF)$_2$[Au(mnt)$_2$] salt, which has a diamagnetic anion, the localized electrons from the donor behave as a two-legged spin ladder system.

[1] To whom correspondence should be addressed. Fax: +34935805729. E-mail: cun@icmab.es.

0022-4596/02 $35.00

On the other hand, the isostructural metallic salts with M = Ni and Pt have two interacting magnetic and conducting subsystems and show antiferromagnetic interactions.

Following the approach of using donors containing peripheral sulfur atoms that promote short S···S interactions, two new families of compounds (BMDT-TTF)$_2$[M(mnt)$_2$] and (EDT-TTF)[M(mnt)$_2$] have been synthesized, where BMDT-TTF = bis(methylenedithio)-tetrathiafulvalene, EDT-TTF = ethylenedithio-tetrathiafulvalene and M = Au, Pt and Ni. The crystal structure and physical characterization has been carried out laying special emphasis on the conducting and magnetic properties which are determined by the charge on the ions.

2. EXPERIMENTAL SECTION

2.1. Synthesis

2.1.1. Synthesis of Starting Materials

The synthesis of the donors BMDT-TTF and EDT-TTF was performed as previously described (7, 8). The (n-Bu$_4$N)[M(mnt)$_2$] salts were also prepared as previously described and purified by recrystallization in acetone–*iso*butanol (9).

2.1.2. Synthesis of the Salts

(BMDT-TTF)$_2$[M(mnt)$_2$] and (EDT-TTF)[M(mnt)$_2$] (M = Au, Ni, Pt) crystals were obtained by electrocrystallization from dichloromethane solutions of the donor and the tetrabutylammonium salt of [M(mnt)$_2$]$^-$ as electrolyte, in approximately stoichiometric amounts, with Pt electrodes and at a constant current of 1 μA. After 1 week, black shiny plate-shaped crystals were obtained.

2.2. Physical measurements

2.2.1. X-ray Crystal Structure Analysis

X-ray data were collected at 223 K, on a Nonius Kappa CCD diffractometer with monochromatic Mo$K\alpha$(λ = 0.71073 Å) radiation. Data were collected via ϕ and ω multiscans and reduced with the program DENZO-SMN without absorption correction. Measured reflections were corrected with the program SCALEPACK. The structure was refined by a full-matrix least-squares method using SHELXL-93. Least-squares calculation minimized $\Sigma w(\Delta F)^2$, being

$$w = [\sigma^2(F_o^2) + (aP)^2 + bP]^{-1}, \quad P = (F_o^2 + 2F_c^2)/3.$$

2.2.2. Transport Measurements

Electrical conductivity and thermoelectric power measurements were performed in the range 175–320 K. In a first step, thermopower was measured using a slow AC ($\sim 10^{-2}$ Hz) technique (10), by attaching to the extremities along the larger dimension of the crystals, with platinum paint (Demetron 308A), two ϕ = 25 mm 99.99% pure Au wires (Goodfellow Metals) anchored to two quartz thermal reservoirs, in a previously described apparatus (11), controlled by a computer (12). The oscillating thermal gradient was kept below 1 K, and it was measured with a differential Au–0.05 atoms% Fe vs chromel thermocouple. The sample temperature was measured by a previously calibrated thermocouple of the same type. The absolute thermopower of the sample was obtained after correction for the absolute thermopower of the Au leads, using the data of Huebner (13).

In a second step, electrical resistivity measurements of the same sample were performed using a four-probe technique. Without removing the crystal from the sample holder, two extra Au wires were placed on the sample in order to achieve a four-in-line contact configuration. Prior to the measurements, the sample was checked for unnested to nested voltage ratio, as defined by Schaeffer *et al.* (14), that was below 5%. Measurements were done imposing through the sample with a current of 1 μA at low frequency (77 Hz) and measuring the voltage drop with a lock-in amplifier. In the larger elongated shaped crystals of (BMDT-TTF)$_2$[Au(mnt)$_2$], it was possible to place four point contacts in a rectangular geometry and measure the anisotropy in the *ab* plane using the Montgomery procedure (15).

2.2.3. EPR spectra

EPR spectra in the range 4–300 K were obtained with an X-Band Bruker ESP 300E spectrometer equipped with a rectangular cavity operating in T102 mode, a Bruker variable temperature unit and an Oxford EPR-900 cryostat, a Field Frequency lock ER 033 M system and a NMR Gaussmeter ER 035 M. The microwave power was kept well below saturation.

2.2.4. Magnetic Susceptibility Measurements

Magnetic susceptibility measurements in the range 2–300 K were performed using a longitudinal Faraday system (Oxford Instruments) with a 7 T superconducting magnet, under a magnetic field of 1, 2 and 5 T and forward and reverse gradients of field of 1 T/m. A polycrystalline sample (6–10 mg) was placed inside a previously calibrated thin-wall Teflon bucket. The force was measured with a microbalance (Sartorius S3D-V). Under these conditions, the magnetization was found to be proportional to the applied magnetic field.

2.2.5. *Electronic Spectroscopy*

Transmission measurements of finely ground KBr pellet samples with a weight concentration about 1% have been carried out with a Nicolet 5ZDX interferometer with fourier transform (400–4400 cm^{-1}) and a Varian Cary5 spectrometer (3330–20,000 cm^{-1}).

3. RESULTS AND DISCUSSION

3.1. Crystal structures

The $(BMDT\text{-}TTF)_2[M(mnt)_2]$ (M = Au, Pt, Ni) salts (16) are quasi-isostructural and crystallize in the triclinic space group $P(-1)$. Their crystallographic data are given in Table 1 and the molecular structure of the Ni salt is depicted in Fig. 1. In these three salts, the $[M(mnt)_2]$ units are essentially planar, whereas the external carbon atoms in the BMDT-TTF molecules are alternately tilted from the mean molecular plane by an angle that ranges from 28° to 40°. In Fig. 2, the projection of the crystal packing of $(BMDT\text{-}TTF)_2[Ni(mnt)_2]$ along c is viewed. The three BMDT-TTF salts crystallize forming mixed stacks in which two molecules of donor alternate with one molecule of the anion (ADDA) along the $a+b$ direction. Additionally, short inter- and intra-dimers S···S contacts between the donor molecules form chains of dimers along a. There are also S···S interactions among the BMDT-TTF molecules along the b and c directions, although they are probably electronically less important as these interactions are mainly involving the external sulfur atoms that have less contribution to the HOMO of the molecule (Fig. 2, Table 2). Finally, we can also find S···S short contacts between the donors and the anions.

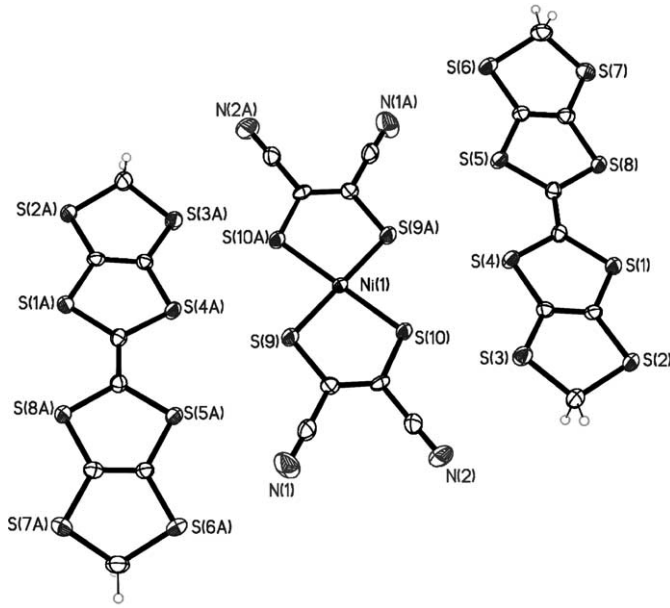

FIG. 1. Molecular structure of $(BMDT\text{-}TTF)_2[Ni(mnt)_2]$.

TABLE 1
Crystallographic Data of $(BMDT\text{-}TTF)_2M(mnt)_2$ and $(EDT\text{-}TTF)M(mnt)_2$ Salts

M	$(BMDT\text{-}TTF)_2$ $[Au(mnt)_2]$	$(BMDT\text{-}TTF)_2$ $[Ni(mnt)_2]$	$(BMDT\text{-}TTF)_2$ $[Pt(mnt)_2]$	$(EDT\text{-}TTF)$ $[Au(mnt)_2]$	$(EDT\text{-}TTF)$ $[Ni(mnt)_2]$	$(EDT\text{-}TTF)$ $[Pt(mnt)_2]$
Formula	$C_{24}H_8S_{20}N_4Au$	$C_{24}H_8S_{20}N_4Ni$	$C_{24}H_8S_{20}N_4Pt$	$C_{16}H_6S_{10}N_4Au$	$C_{16}H_6S_{10}N_4Ni$	$C_{16}H_6S_{10}N_4Pt$
Molecular mass	1190.51	1052.25	1188.63	771.81	633.56	769.94
T(K)	223(2)	223(2)	223(2)	223(2)	223(2)	223(2)
Dimensions (mm)	$0.3\times0.15\times0.015$	$0.4\times0.2\times0.1$	$0.25\times0.2\times0.01$	$0.15\times0.11\times0.01$	$0.25\times0.12\times0.02$	$0.2\times0.1\times0.01$
Crystal system	Triclinic	Triclinic	Triclinic	Triclinic	Monoclinic	Monoclinic
Space group	P-1 (No. 2)	P-1(No. 2)	P-1 (No. 2)	P-1 (No. 2)	$C2/c$ (No. 15)	$C2/c$ (No. 15)
a (Å)	7.9890(3)	7.9748(3)	8.0431(3)	8.7913(3)	12.8018(7)	12.8875(7)
b (Å)	9.0629(3)	8.5611(4)	8.4565(6)	11.6689(6)	25.654(1)	25.848(2)
c (Å)	12.6676(5)	12.8436(6)	12.9562(9)	17.1061(8)	7.8666(5)	7.8685(5)
α (deg)	92.882(2)	90.344(3)	89.835(3)	100.949(2)	90	90
β (deg)	94.161(2)	91.196(2)	90.696(4)	97.141(2)	120.172	120.292
γ (deg)	96.189(2)	95.762(3)	95.508(4)	96.229(3)	90	90
Volume (Å^3)	907.87(6)	872.22(7)	877.10(9)	1693.72(13)	2233.5(2)	2263.3(3)
Z	1	1	1	3	4	4
ρ_{calc}($g\cdot cm^{-3}$)	2.178	2.003	2.250	2.270	1.884	2.260
Intervals h, k, l	0–8, ±9, ±13	0–9, ±10, ±15	0–8, ±9, ±14	0–9, ±12, ±18	0–14, ±28, −8–7	0–14, ±28, −8–7
$2\theta_{max}$ (deg)	46	42	42	45	42	42
Reflections collected	4714	3239	3375	7968	4529	4133
Independent reflections	2514	1849	1879	4434	1288	1210
Reflections > $2\sigma(I)$	2476	1754	1824	3491	1156	1078
R_1	0.0240	0.0343	0.0538	0.0440	0.0365	0.0822
wR_2	0.0601	0.0868	0.1346	0.1009	0.0943	0.1950

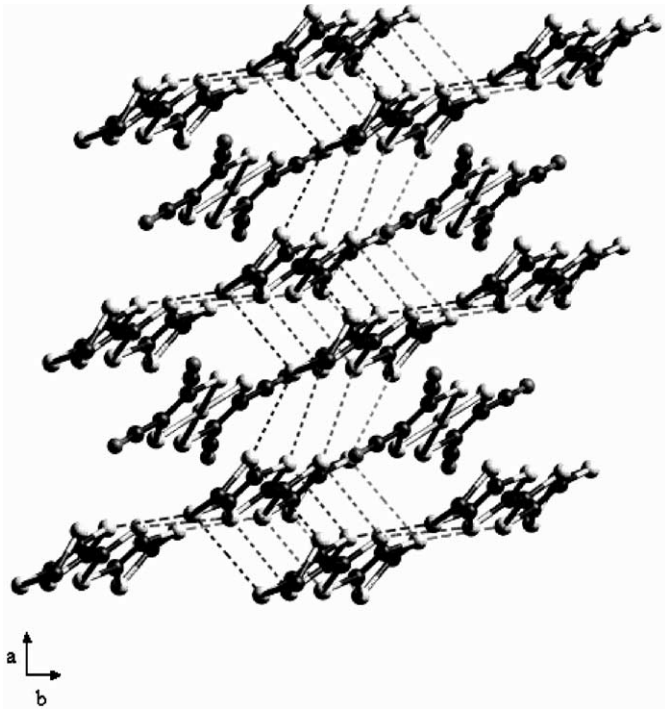

FIG. 2. Projection of the crystal structure of the (BMDT-TTF)$_2$[Ni(mnt)$_2$] salt along the *c*-axis showing the short S···S contacts.

We focus now on the crystal structures of (EDT-TTF)[*M*(mnt)$_2$] (*M* = Au, Pt, Ni). Their molecular structures are shown in Fig. 3a and b where it can be seen that whereas in the Ni and Pt salts there is no disorder of the asymmetric donor, the orientation of the EDT-TTF molecules in the Au salt is 50% disordered along the long axis of the molecule. The crystallographic data are given in Table 1 where it can be seen that the salts with Ni and Pt are isostructural and crystallize in the monoclinic space group *C*2/*c*. These two salts crystallize forming alternated stacks of molecules of EDT-TTF and [*M*(mnt)$_2$] along *c* (Fig. 4). This structure is stabilized because the –CN groups from the anions promote two types of N···H–C interactions with the neighboring EDT-TTF molecules in the direction of the *b*-axis. The corresponding distances and angles ((EDT-TTF)[Ni(mnt)$_2$]: **a**: N···C = 3.331 Å, θ(C–H···N) = 169°; **b**: N···C = 3.551 Å, θ(C–H···N) = 169°; (EDT-TTF)[Pt(mnt)$_2$]: **a**: N···C = 3.366 Å, θ(C–H···N) = 168°; **b**: NC = 3.585 Å, θ(C–H···N) = 168°) indicate that they correspond to intermolecular hydrogen bonds (Fig. 4b). There are also short S···S intra-stack (3.790 Å < SS < 3.980 Å) and inter-stack (3.481 Å < S···S < 3.885 Å) interactions. In addition, we can notice that in each stack the donor molecules have the same orientation but, considering the neighboring stacks, they are orientated head-to-tail (Fig. 4b).

The (EDT-TTF)[Au(mnt)$_2$] salt crystallizes in the triclinic space group *P*(-1). This salt forms also alternated stacks along *a*. There are two different alternated stacks, named A and B, considering their orientation with respect to the stacking *a* axis, that appear in a sequence ABBA (Fig. 5). The A and B stacks form an angle of 50° between them. There are short S···S intra-stack contacts (3.60–3.98 Å) and also S···S inter-stacks interactions between A and B stacks (3.57–3.89 Å).

3.2. Optical properties and determination of the charge on the ions

The stoichiometry of the salts (BMDT-TTF)$_2$[*M*(mnt)$_2$] and (EDT-TTF)[*M*(mnt)$_2$] where found to be 2:1 and 1:1, respectively, by X ray. However, in order to determine the oxidation state of the donors, we should take into account that, in some cases, when the anion has an acceptor character some charge transfer from the donor to the anion can take place during the electrocrystallization process (17). Since [*M*(mnt)$_2$]$^-$ (*M* = Ni, Pt) ions are good acceptors (18), it is necessary to find out if the monoanionic character of the anions has remained unaltered. Best *et al*. studied the relationship between the stretching modes of CN groups (ν(CN)) and the charge (−1 to −3) of the [*M*(mnt)$_2$]$^{n-}$ complexes (19). In [*M*(mnt)$_2$]$^{n-}$ salts, the CN groups give rise to intense vibrational bands which are in general only weakly coupled to other vibrations of the molecule, and are well isolated from the vibrational modes of the donor molecule. These bands can therefore, be used for the determination of the valence of the anion complex. It has been found that the ν(CN) increases by about $15 \pm 1\ cm^{-1}$ upon oxidation from the dianion to the monoanion (Table 3). On the other hand, it is also well known that

TABLE 2
S···S Short Distances in the (BMDT-TTF)$_2$[*M*(mnt)$_2$] Salts

Distances S···S (Å)	(BMDT-TTF)$_2$[Au(mnt)$_2$]	(BMDT-TTF)$_2$[Ni(mnt)$_2$]	(BMDT-TTF)$_2$[Pt(mnt)$_2$]
Intra-dimer	3.564, 3.594, 3.937, 3.952	3.395, 3.405, 3.819, 3.861	3.406, 3.415, 3.842, 3.877
Inter-dimer along *a*	3.557, 3.649, 3.904	3.468, 3.636, 3.893	3.486, 3.674, 3.887
Inter-dimer along *b*	3.622, 3.834	3.439, 3.688	3.429, 3.699
Inter-dimer along *c*	3.644	3.494, 3.720	3.609, 3.778
BMDT-TTF···[*M*(mnt)$_2$]	3.513, 3.590, 3.559, 3.723, 3.796, 3.892, 3.894, 3.954, 3.996	3.439, 3.492, 3.526, 3.563, 3.564, 3.818, 3.855, 3.883, 3.916,	3.438, 3.480, 3.508, 3.587, 3.635, 3.821, 3.829, 3.890, 3.901

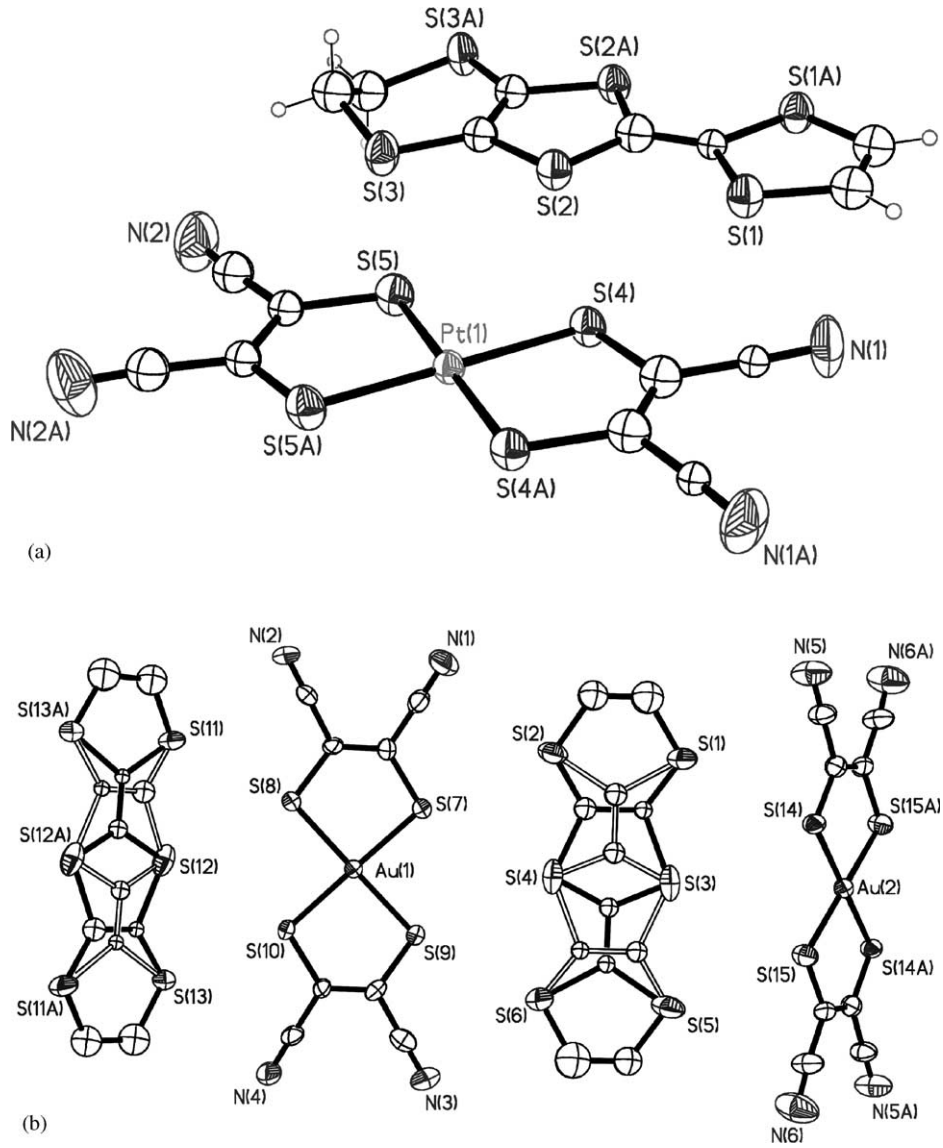

FIG. 3. Molecular structure of (a) (EDT-TTF)Pt$(\text{mnt})_2$ (the Ni salt is isostructural) and (b) (EDT-TTF)Pt$(\text{mnt})_2$ showing the 50% disorder of the EDT-TTF molecule along the longer molecular axis.

the molecular geometry varies with the electron population of the MOs in the complexes (19). Thus, a comparison of the M–S bond lengths in neutral $[M(\text{mnt})_2]$, $[M(\text{mnt})_2]^-$, and $[M(\text{mnt})_2]^{2-}$ species reveals that this parameter is also very sensitive to the oxidation state of the metal, although it should be kept in mind that the relation between charge transfer and geometry is approximate (4, 17, 19–28).

Comparing the ν(CN) stretching mode values and the M–S bond distances in the salts based on BMDT-TTF and EDT-TTF with those of other well-characterized $[M(\text{mnt})_2]^{n-}$ salts (Table 3), we can conclude that the anions in the EDT-TTF donor derivatives and in the (BMDT-TTF)$_2$Au$(\text{mnt})_2$ salt have a formal charge of nearly –1. Contrary, the frequencies and distances obtained for the salt (BMDT-TTF)$_2$[Ni$(\text{mnt})_2$] point towards a formal charge of -2 on the [Ni$(\text{mnt})_2$] complex. The analysis of the central C=C and C–S bond lengths of the donors in the different salts, that also are sensitive to the charge of the molecule (29), agree with the charges assigned to them. Thus following the equation developed by BEDT-TTF donor (29) BMDT-TTF gave an average δ value of 0.782 for the Au salt and of 0.724 for the Ni salt which are near the values for formal charges of $+0.5$ and $+1$ respectively. Regarding the EDT-TTF salts, the δ values are 0.695, 0.714 and 0.689 for Au, Ni and Pt salts, which correspond to a charge of $+1$.

In accordance with the above-mentioned results, in the Vis/NIR spectra of the EDT-TTF-based salts and

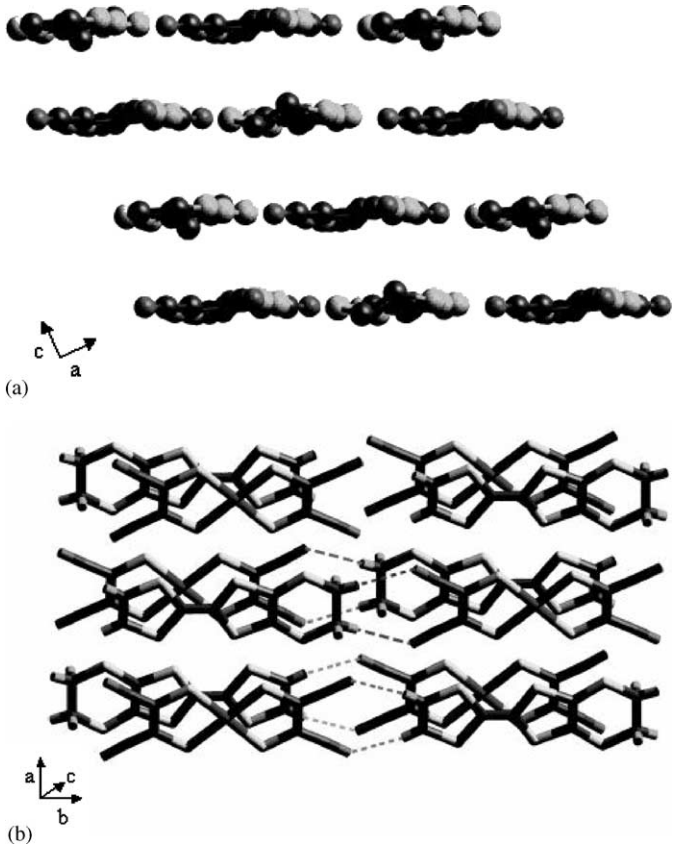

FIG. 4. (a) Projection of the crystal packing of the (EDT-TTF)[Pt(mnt)$_2$] salt along the *b*-axis. (b) View of two layers of (EDT-TTF)[Pt(mnt)$_2$] salt in the *ab* plane showing the N$\cdots$C–H interactions.

(BMDT-TTF)$_2$Ni(mnt)$_2$, no A bands corresponding to the mixed-valence states of low dimensional organic solids were observed (30). This is due to the fact that the oxidation state of the donor in these salts is +1, that is to say, the salts are completely ionic. In the (BMDT-TTF)$_2$Au(mnt)$_2$ salt, the donor molecules have a formal charge of +0.5 and this salt exhibits an A band centerd at 3500 cm^{-1} in its Vis/NIR spectra.

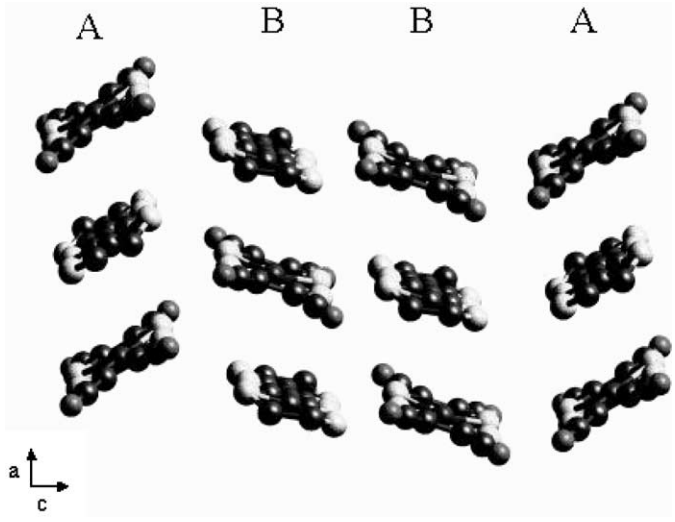

FIG. 5. Projection of the crystal packing of the (EDT-TTF)[Au(mnt)$_2$] salt along the *b*-axis.

3.3. Magnetic properties

Since the [Au(mnt)$_2$]$^-$ and [Ni(mnt)$_2$]$^{2-}$ anions are diamagnetic, the magnetic properties of the corresponding (BMDT-TTF)$_2$[*M*(mnt)$_2$] salts result from the spins on the BMDT-TTF dimer chains. The plot of the static paramagnetic susceptibility with temperature (χ_pT) vs *T* of these salts, measured by the Faraday method in the range 2–300 K and assuming a diamagnetic contribution of 4.98×10^{-4} and 4.96×10^{-4} emu/mol (estimated from tabulated Pascal constants), respectively, is shown in Fig. 6. The value of χ_pT at room temperature in the (BMDT-TTF)$_2$[Au(mnt)$_2$] salt clearly indicates that there is one spin per formula unit and, moreover, that the electrons in the BMDT-TTF units are already localized at this temperature, in agreement with the transport properties shown below. One can consider as the spin carrier units in this Au salt those formed by dimerized donors (BMDT-TTF)$_2^{+\cdot}$, with spin $\frac{1}{2}$. Following the structural interactions such dimerized donors can interact magnetically with the neighboring spin carrier units along *a* giving rise to a 1D antiferromagnetic chain motif. Along the other two directions, there are also interactions arising from the lateral S$\cdots$S short contacts but they are weaker. In agreement with the previous considerations, the magnetic data can be fitted to the Heisenberg model (31) modified with a molecular field with $J_1/K_B = -29.5$ K and $J_2/K_B = -11.1$ K ($r^2 = 0.999$).

In the (BMDT-TTF)$_2$[Ni(mnt)$_2$] all the donor molecules have spin2. Thus, the magnetic interactions will take place basically along the dimer chains. Moreover, the low χ_pT value at room temperature proves the presence of strong antiferromagnetic interactions. As shown in Fig. 6, its susceptibility can be fitted to a Curie–Weiss law over all temperature range (2–300 K) with a high-negative Weiss constant –273 K ($r^2 = 0.998$). Attempts to fit the susceptibility data with a simple 1D antiferromagnetic alternated chain model failed (32), showing that the dimers do indeed further interact along the other directions in the solid.

The EPR spectra of (BMDT-TTF)$_2$[Au(mnt)$_2$] and (BMDT-TTF)$_2$[Ni(mnt)$_2$] salts confirm the diamagnetic character of the anions as they only display a narrow EPR signal with *g*-values typical of the organic donor. The (BMDT-TTF)$_2$[Ni(mnt)$_2$] salt display a very weak EPR signal in accordance with the existence of strong antiferromagnetic interactions. The dependence of the signal intensities with temperature follows the same behavior as found for the susceptibility measurements and no

TABLE 3
CN Stretching Frequency, *M*–S Bond Lengths and Anion Charge of $[M(mnt)_2]^{n-}$ Based Salts

Anion	Cation	ν(CN) cm^{-1}	d (*M*–S) Å	Anion charge	Ref.
$Au(mnt)_2$	Solution	2213, 2226		−1	(19)
		2195		−2	(19)
	Bu_4N	2208, 2222		−1	(19)
	Et_4N		2.307, 2.305, 2.312,		(34)
			2.300,2.308, 2.309	−1	
	Perylene		2.308, 2.322	−1	(6)
	BET-TTF[a]	2222	2.308, 2.302	−1	(17)
	NMPZ[b]		2.327, 2.310, 2.316		
	DT-TTF	2204, 2216	2.317, 2.320	−1	(6)
	BMDT-TTF	2208, 2222	2.312, 2.310	−1	This work
	EDT-TTF	2208, 2222	2.300, 2.309, 2.314,	−1	This work
			2.316		
$Ni(mnt)_2$	Solution	2211, 2226(sh)		−1	(19)
		2195, 2213(sh)		−2	(19)
	Bu_4N	2206, 2220(sh)		−1	(18)
		2197, 2216(sh)		−2	(19, 21)
	Et_4N	2194(sh), 2210	2.148, 2.151,2.149	−1	(19, 35)
		2195, 2205(sh)	2.177, 2.171	−2	
	Perylene		2.146, 2.135	−1	(6)
	NMPZ[b]		2.142, 2.141, 2.139,	−1	(36)
			2.134, 2.137		
			2.158, 2.175	−2	(37)
	DT-TTF	2205	2.144, 2.155	−1	(6)
	BMDT-TTF	2212, 2193	2.175, 2.2176	−2	This work
		2177			
	EDT-TTF	2208	2.144, 2.143	−1	This work
$Pt(mnt)_2$	Solution	2208	2.144, 2.143	−1	This work
		2204(sh), 2215		−1	(19)
		2189(sh), 2200		−2	(19)
	Bu_4N	2207	2.262, 2.256, 2.265,	−1	(6, 38)
		2188(sh), 2197	2.290, 2.282	−2	(19, 28)
	Et_4N		2.261, 2.274, 2.270	−1	
			2.259		
	Perylene	2207	2.262, 2.260	−1	(6)
	BET-TTF[a]	2194, 2181(sh)		−2	(17)
	DT-TTF	2205.0	2.269, 2.275	−1	(6)
	EDT-TTF	2210	2.265, 2.244	−1	This work

[a] Bisethylenethio-tetrathiafulvalene.
[b] *N*-Methylphenazinium.

important changes in its parameters were observed, revealing that there are no phase transitions. The EPR parameters (g factor and peak-to-peak line width (ΔH_{pp}) of the EPR spectra performed in single crystals at room temperature are collected in Table 4. We should notice that the minimum g value observed for these salts is close to the free electron value of 2.0023, as expected for any planar sulfur π-donor radical cation with the axis perpendicular to the molecular plane oriented parallel to the applied magnetic field, where the contribution of the spin–orbit coupling is very small (33).

In the (EDT-TTF)$[M(mnt)_2]$ (M = Ni, Pt) salts, the anions are paramagnetic (square-planar Ni^{III} and Pt^{III} complexes have a spin $\frac{1}{2}$) and, therefore, their magnetic properties have two different contributions coming from the donor molecules and the anionic complexes. The plot of χ_pT vs T of (EDT-TTF)$Pt(mnt)_2$, considering a diamagnetic contribution of 2.88×10^{-4} emu/mol, is depicted in Fig. 7, in which it can be seen that antiferrromagnetic interactions predominate. Accordingly to the crystal structures, the magnetic interactions follow a 1D chain motif. Data for both (EDT-TTF)$M(mnt)_2$ (M = Ni, Pt) salts are satisfactorily fitted to the antiferromagnetic uniform chain model of Heisenberg (32). Considering a small diamagnetic contribution of 2.8×10^{-5} emu/mol, we find $J/K_B = -7.5$ K for (EDT-TTF)$Pt(mnt)_2$ ($r^2 = 0.998$) and $J/K_B = -9.0$ K for (EDT-TTF)$Ni(mnt)_2$ ($r^2 = 0.995$).

The EPR spectra obtained for (EDT-TTF)$Ni(mnt)_2$ and (EDT-TTF)$Pt(mnt)_2$ display one very broad signal with a g factor of 2.0460 and 1.9062 and a line width of 960

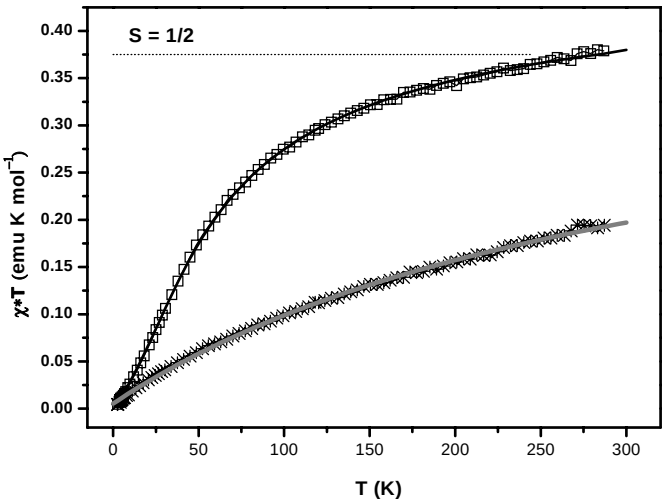

FIG. 6. Temperature dependence of $\chi_p T$ of (BMDT-TTF)$_2$[M(mnt)$_2$] with M = Au (□) and M = Ni (∗). The solid lines are the fits by 1D antiferromagnetic Heisenberg model modified with a molecular field for the salt with M = Au and by the Curie–Weiss law for the salt with M = Ni.

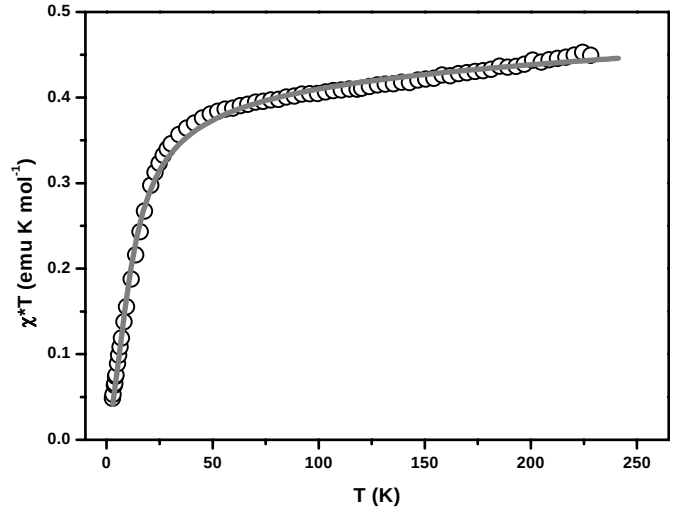

FIG. 7. Temperature dependence of $\chi_p T$ of (EDT-TTF)Pt(mnt)$_2$. The solid line is the fit by 1D antiferromagnetic Heisenberg model.

and 930 G, respectively. This indicates that there are interactions between the two paramagnetic units. With decreasing temperature, the line widths remain practically constant but the g factor diminishes.

The EPR parameters of a single crystal of (EDT-TTF)[Au(mnt)$_2$] salt are listed in Table 4 and are consistent with the diamagnetic character of the [Au(mnt)$_2$]$^-$ anion.

3.4. Electrical transport properties

As expected from the alternated stacking structure of the (BMDT-TTF)$_2$[M(mnt)$_2$] compounds, their electrical conductivity is relatively low and typical of semiconductors.

The (BMDT-TTF)$_2$[Au(mnt)$_2$] salt has an electrical conductivity at room temperature of 3.9×10^{-3} S/cm which presents a semiconducting behavior with an activation energy of 0.20 eV (Fig. 8a). The longest dimension of the crystal used for these measurements was found by X-ray diffraction to be $a+b$. However, the anisotropy measurements made by the Montgomery technique indicate that the anisotropy of the electrical conductivity in the *ab* plane is smaller than 2 and in view of the crystal structure a semiconducting behavior, almost isotropic in this plane, is expected. This low conductivity value is consistent with the high localization of the spins on the dimers as seen in magnetic properties. Thermopower, S, is positive in the whole temperature range studied (300–175 K) (Fig. 8b) increasing upon cooling thus confirming the semiconducting behavior.

For (BMDT-TTF)$_2$[Ni(mnt)$_2$], the room temperature conductivity was found to be 8.8×10^{-4}S/cm. This value is only slightly smaller than that of the Au compound, but the electrical conductivity presents a more drastic decrease upon cooling, corresponding to a semiconducting regime with a larger activation energy of 0.31 eV (Fig. 8a). In this case, the thermopower measured only at room temperature presents large negative values (−740 μV/K). This difference in the thermopower values, from positive in the Au compound to negative in the Ni one, is a consequence of the full ionic nature of the Ni salt.

TABLE 4
EPR Parameter of the (BMDT-TTF)$_2$Au(mnt)$_2$, (BMDT-TTF)$_2$Ni(mnt)$_2$ and (EDT-TTF)Au(mnt)$_2$

		(BMDT-TTF)$_2$ [Au(mnt)$_2$]	(BMDT-TTF)$_2$ [Ni(mnt)$_2$]	(EDT-TTF) [Au(mnt)$_2$]
Maximum	g	2.0114	2.0143	2.0139
	ΔH_{pp} (G)	9.15	6.7	27.0
Intermediate	g	2.0085	2.0076	2.0053
	ΔH_{pp} (G)	7.29	5.2	20.2
Minimum	g	2.0010	2.0024	2.0008
	ΔH_{pp} (G)	6.86	5.0	20.1

4. CONCLUSIONS

To summarize, two new families of charge transfer salts based on maleonitrile dithiolate (mnt)–metal (M) complexes and the π-electron donors BMDT-TTF and EDT-TTF have been synthesized by electrochemical means and characterized. These two donors incorporate external sulfur atoms that promote S · · · S contacts providing either donor–donor or donor–anion interactions and, hence, dimensionality enhancement in the structure. In addition, the CN groups from the anions can also give rise to hydrogen bonding interactions that stabilize the crystal

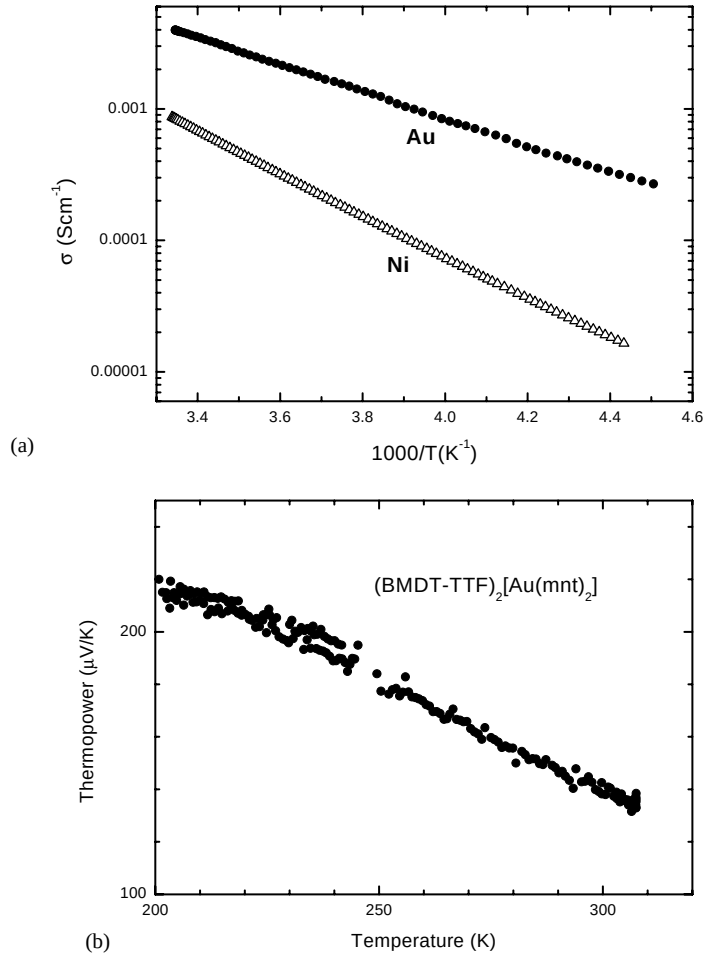

FIG. 8. Transport properties of (BMDT-TTF)$M(\mathrm{mnt})_2$: (a) logarithm of the electrical resistivity as a function of the reciprocal temperature, (b) thermoelectric power as function of temperature.

structures. We have used both diamagnetic (M = Au) and paramagnetic (M = Ni, Pt) counterions to obtain compounds in which delocalized conduction electrons and non-magnetic or localized magnetic centres can co-exist. However, since the anions with M = Ni are good acceptors, sometimes some charge transfer from the donor to the anion occurs during the electrocrystallization, which gives rise to a non-magnetic $[\mathrm{Ni(mnt)_2}]^{2-}$ anion and determines the resulting electrical and magnetic properties of the salts.

In the $(\mathrm{BMDT\text{-}TTF})_2[\mathrm{Au(mnt)_2}]$, the anion has a formal charge of –1 and is diamagnetic, thus, it is a mixed-valence salt which reveals a semiconducting behavior. Its magnetic susceptibility can be fitted to a 1D antiferromagnetic chain model considering the dimerized donors $(\mathrm{BMDT\text{-}TTF})_2^+$ as the spin carrier units. However, in the $(\mathrm{BMDT\text{-}TTF})_2[\mathrm{Ni(mnt)_2}]$ salt, there is a formal charge of –2 on the anion. The magnetic properties in this latter salt come also from the donor molecules, which are completely oxidized, and exhibit strong 3D antiferromagnetic interactions. It is interesting to mention that these two charge transfer salts are one of the few examples in which the same crystal structure is found even though there is a large change in the charge of constituent molecules.

In the (EDT-TTF)$[M(\mathrm{mnt})_2]$ (M = Au, Ni, Pt) salts, all the anion complexes have a charge of –1 being, therefore, completely ionic salts. The magnetic properties of the Ni and Pt salts have two different contributions arising from the electrons on the donor and the anion molecules, and follow a uniform 1D antiferromagnetic chain motif.

Further work will concentrate on preparing new salts using different π-electron donors, especially, those containing some aromatic substituents that seem to be more appropriate for our aim of obtaining more compounds that are able to combine electrical and magnetic properties.

ACKNOWLEDGMENTS

This work was partially supported by Comisión Interministerial de Ciencia y Tecnología (MAT2000-1388-C03-01 and BQU2000-1157) and

Generalitat de Catalunya (2000SGR-00114) (Spain) and by Fundação para a Ciência e Tecnologia (Portugal) under Contracts POCTI/1999/Qui/35452. The collaboration between the team members of Sacavém and Barcelona was supported under the CSIC-ICCTI bilateral agreement and by COST action D14/0003/99.

REFERENCES

1. F. Wudl, *Acc. Chem. Res.* **17,** 227 (1984); *in* "Highly Conducting Quasi-One-Dimensional Organic Crystals, Semiconductors and Semimetals" E. Conwell, Ed. Vol. 27. Academic Press, Inc., London, 1988; *in* "The Physics and Chemistry of Organic Superconductors" G. Saito and S. Kagoshima, Eds. Springer, Berlin, 1990; J. M. Williams, J. R. Ferraro, R. J. Thorn, K. D. Carlson, U. Geiser, H. H. Wang, A. M. Kini, and M.-H. Whangbo, "Organic Superconductors, Including Fullerenes: Synthesis, Structure, Properties, and Theory." Prentice-Hall, Englewood Cliffs, NJ, 1992; in "Organic Conductors; Fundamentals and Applications" (J.-P. Farges. Ed. Marcel-Dekker Inc., New York, 1994.
2. A. W. Graham, M. Kurmoo, P. Day, *J. Chem. Soc. Chem. Commun.* 2061 (1995); M. Kurmoo, A. W. Graham, P. Day, S. J. Coles, M. B. Hursthouse, J. L. Caufield, J. Singleton, F. L. Pratt, W. Hayes, L. Ducasse, and P. Guionneau, *J. Am. Chem. Soc.* **117,** 12,209 (1995).
3. E. Coronado, J. R. Galán-Mascarós, C. J. Goméz-García,V. Laukhin, *Nature* **408,** 447 (2000); E. Coronado, J. R. Galán-Mascarós, C. Jiménez-Sainz, and C. J Gómez-García, *Adv. Mater. Opt. Electron.* **8,** 61 (1998).
4. L. Alcácer, H. Novais, F. Pedroso, S. Flandrois, C. Coulon, D. Chasseau, J. Gaultier, *Solid State Commun.* **35,** 945 (1980); V. Gama, M. Almeida, R. T. Henriques, I. C. Santos, A. Domingos, S. Ravy, and J. P. Pouget, *J. Phys. Chem.* **95,** 4263 (1991); V. Gama, I. C. Santos, G. Bonfait, R. T. Henriques, M. T. Duarte, J. C. Waerenborgh, L. Pereira, J. M. P. Cabral, and M. Almeida, *Inorg. Chem.* **31,** 2598 (1992).
5. A. Domingos, R. T. Henriques, V. Gama, M. Almeida, A. L. Vieira, and L. Alcacer, *Synth. Met.* **27,** B411 (1988)
6. C. Rovira, J. Veciana, E. Ribera, J. Tarrés, E. Canadell, M. Mas, E. Molins, M. Almeida, R. T. Henriques, J. Morgado, J.-P. Schoeffel, and J.-P. Pouget, *Angew. Chem. Int. Ed. Engl.* **36** (21), 2324 (1997); E. Ribera, C. Rovira, J. Veciana, J. Tarrés, E. Canadell, R. Rousseau, E. Molins, M. Mas, J.-P. Schoeffel, J.-P. Pouget, J. Morgado, R. T. Henriques, and M. Almeida *Chem. Eur. J.* **5**(7), 1067 (1999).
7. R. Kato, A. Kobayashi, Y. Sasaki, and H. Kobayashi, *Chem. Lett.* 993 (1984).
8. R. K. Boeckman, *Org. Synth.* **73,** 270 (1995).
9. A. Davison, N. Edelstein, R. H. Holm, A. H. Maki, *Inorg. Chem.* **2,** 1227 (1963); A. Davison and R. H. Holm, *Inorg. Synth.* **10,** 8 (1967).
10. P. M. Chaikin and J. F. Kwak, *Rev. Sci. Instrum.* **46,** 218 (1975).
11. M. Almeida, S. Oostra, L. Alcácer, *Phys. Rev. B* **30,** 2839 (1984).
12. E. B. Lopes, "INETI- Sacavem." Internal Report, 1991.
13. R. P. Huebner, *Phys. Rev. A* **135,** 1281 (1964).
14. P. E. Schaffer, F. Wudl, G. A. Thomas, J. P. Ferraris, and D. O. Cowan, *Solid State Commun.* **14,** 347 (1974).
15. H. C. Montgomery, *J. Appl. Phys.* **42,** 2971 (1971).
16. The crystal structure of the $(BMDT\text{-}TTF)_2[Pt(mnt)_2]$ is from one crystal of the material synthesized but we cannot attribute this crystal's structure to all crystals obtained since it seems that different phases are formed in the same electrocrystallization. We are currently further working in the full characterization of this salt.
17. J. Tarrés, M. Mas, E. Molins, J. Veciana, C. Rovira, J. Morgado, R.T. Henriques, and M. Almeida, *J. Mater. Chem.* **5,** 1653 (1995).
18. Cyclic voltammetry of the starting tetrabutylammonium salts gives $E_{1/2}$ for $Pt(mnt)_2^- \leftrightharpoons Pt(mnt)_2^{2-} = 0.32\,V$ and for $Ni(mnt)_2^- \rightleftharpoons Ni(mnt)_2^{2-} = 0.35\,V$ vs Ag/AgCl in CH_2Cl_2.
19. S. P. Best, S. A. Ciniawsky, R. J. H. Clark, R. C. S. McQueen, *J. Chem. Soc. Dalton Trans.* 2267 (1993).
20. T. C. Umland, S. Allie, T. Kuhlmann, and P. Coppens, *J. Phys. Chem.* **92,** 6456 (1988).
21. A. Kobayashi, and Y. Sasaki, *Bull. Chem. Soc. Jpn.* **50,** 2650 (1977).
22. W. Reith, K. Polborn, and E. Amberger, *Angew. Chem. Int. Ed. Engl.* **27,** 699 (1988).
23. I. G. Dance, P. J. Solstad, and J. C. Calabrese, *Inorg. Chem.* **12,** 2161 (1973).
24. F. Knoch, G. Schmauch, and H. Kisch, *Z. Kristallogr.* **210,** 76 (1995).
25. P. I. Clemenson, A. E. Underhill, M. B. Hursthouse, and R. L. Short, *J. Chem. Soc. Dalton Trans.* 61 (1989).
26. J. S. Miller, J. C. Calabrese, and A. J. Epstein, *Inorg. Chem.* **28,** 4230 (1989).
27. W. Clegg, S. L. Birkby, A. J. Banister, J. M. Rawson, S. T. Wait, P. Rizkallah, M. M. Harding, and A. Blake, *Acta Crystallogr.* **50,** 28 (1994).
28. W. Guntner, G. Gliemann, U. Klement, M. Zabel, *Inorg. Chim. Acta* **165**, 51 (1989).
29. P. Guionneau, C. J. Kepert, G. Bravic, D. Chasseau, M. R. Truter, M. Kurmoo, and P. Day, *Synth. Met.* **86,** 1973 (1997).
30. J. B. Torrance, B. W. Scott, F. B. Kaufman, and P. E. Seiden, *Phys. Rev. B* **19,** 730 (1979).
31. W. E. Hatfield, W. E. Estes, W. E. Marsh, M. W. Pickens, L. W. Ter Haar, R. and R. Weller, in Extended Chain Compounds" (J. S. Miller, Ed.), Vol. 3, p. 45. Plenum Press, New York, 1982.
32. T. Barnes, J. Riera, *Phys. Rev. B* **50**(10), 6817 (1994).
33. A. Terahara, H. Ohya-Nishigushi, N. Hirota, H. Awaji, T. Kawase, S. Yoneda, T. Sugimoto, and Z. Yoshida *Bull. Chem. Soc. Jpn.* **57,** 1760 (1984).
34. J. C. Fitzmaurice, A. M. Z. Slawin, D. J. Williams, and J. D. Woollins, *Polyhedron* **9,** 1561 (1990).
35. C. Mahadevan, M. Seshasayee, B.V. Murthy, P. Kuppusamy, and P.T. Manoharan, *Acta Crystallogr. C* **40,** 2032 (1984).
36. F. Kuppusamy, N. Venkatalakshmi, and P. T. Manoharan, *J. Crystallogr. Spectrosc. Res.* **15,** 389 (1985).
37. H. Endres, H. J. Keller, W. Moroni, and D. Nothe, *Acta Crystallogr. B* **35,** 353, (1979).
38. R. Kirmse, and S. Saluschke, Private Communication, 1996.